COMPARATIVE CHARACTERIZATIONS OF THE ICE NUCLEUS ABILITY OF AgI AEROSOLS BY THREE METHODS

Paul J. DeMott[a], Arlin B. Super[b], Gerhard Langer[c], David C. Rogers[a] and Jack T. McPartland[b]

[a] Department of Atmospheric Science
Colorado State University
Fort Collins, CO

[b] U.S. Bureau of Reclamation
Denver, CO

[c] Boulder , CO

Abstract. Three methods were used to assess the ice nucleating ability of different AgI-based aerosols produced using two solution combustion generators. The standard method employed was an isothermal cloud chamber which has been historically used for "calibrations" of ice nucleus aerosol generators. Comparisons with historical data showed consistency over a 20 year period for one generator, but not for another. Data on rates of ice crystal formation were used to infer operative ice formation mechanisms, and make inferences to the relative utility of the different aerosols in the atmosphere. Comparative measurements of ice nucleus effectiveness at -20°C were made using two NCAR counters that have been used operationally to trace the aerosols tested. Results showed that these devices can give self-consistent results and typically measure about 33% of the ice nuclei measured in the larger cloud chamber and 25% of the total AgI aerosols present. These results varied depending on the ice nucleus aerosol tested, presumably due to differences in particle size and chemistry. Measurements of the ice-forming ability of one aerosol ($AgCl_{0.22}I_{0.78}$-0.125NaCl) were also made with a continuous flow ice-thermal diffusion chamber. These measurements showed that the water supersaturation dependence of the ice formation rate by condensation-freezing for these aerosols varies by more than three orders of magnitude between 0 and 7% supersaturation. Ice formation was nearly instantaneous above 7% supersaturation for all aerosols capable of acting as ice nuclei. The various measurements taken will permit the quantitative transfer of laboratory results on ice nucleus ability to a range of expected atmospheric conditions.

1. INTRODUCTION

A laboratory characterization of the ice nucleating ability of aerosols produced from burning silver iodide (AgI) based solutions in two solution combustion cloud seeding generators used in the Utah/NOAA Atmospheric Modification Program (AMP) was made at the Colorado State University (CSU) Cloud Simulation and Aerosol Laboratory (hereafter referred to as Sim Lab). The primary characterization was made using historical procedures. Namely, the CSU vertical dilution wind tunnel was used as an aerosol generation plenum and the isothermal cloud chamber (ICC) as the basis for effectiveness determination. This testing program afforded the opportunity to examine the consistency of results of ice formation effectiveness made 13 and 22 years previously with the same or similar cloud seeding generators. An analysis of ice formation rates and mechanisms was also undertaken following the procedures of DeMott et al. (1983).

In association with the cloud chamber testing, comparative measurements were made of ice nucleating effectiveness using two NCAR ice nucleus (IN) counters that were previously deployed for tracking ice nucleus transport and dispersion over the Wasatch Plateau of central Utah. The purpose of these comparative measurements was to be able to relate the NCAR counter measurements in the field to a quantitative ice nucleus aerosol concentration and to a predicted ice nucleation effectiveness based on the cloud chamber calibrations (e.g., Super and Holroyd, 1994). A previous laboratory study of this

type (Sackiw et al., 1984) had stated that in addition to the factor of 10 correction for ice crystal detection efficiency (Langer, 1973), NCAR counter concentration values were as much as another factor of 10 lower than ICC-measured effectiveness for certain AgI aerosols and varied depending on the nucleant chemistry. This was presumably due to differences in ice formation mechanisms and residence times in the two measurement methods. The aerosols used in the earlier studies were AgI•0.5NaI aerosols produced by burning impregnated-coke and very small AgI aerosols produced by arcing electricity between solid AgI electrodes. These results may not be generally applicable to measuring other nucleant types, such as ones generated by combustion of solutions.

An additional comparative study of ice formation ability was made using the continuous flow diffusion chamber (CFD) described by Rogers (1988; 1994). This instrument may be of great utility for tracing ice nucleus aerosols in the atmosphere. It permits the independent control of both temperature and humidity. This allowed for a preliminary study of the effects of saturation ratio on ice formation by one AgI aerosol.

2. LABORATORY METHODS

2.1 IN Aerosol Generation

Standard procedures for testing ice nucleus generators at the Sim Lab (see, e.g., Garvey, 1975) include the use of a vertical wind tunnel to simulate operational conditions of air flow rate and mixing for the generator being tested. A sample of the aerosol is taken from the tunnel at 8 m downstream of solution combustion generators using a 4.25 liter syringe. The mass concentration of nucleant in the syringe is calculated using the generator nucleant burn rate (g min^{-1}), and the tunnel air flow rate (l min^{-1}). The sample is sometimes diluted further by expelling a portion of the sample air from the syringe and replacing it with particle-free, dry air. Each dilution reduces the number of aerosols in the syringe by a factor of 8.64. This procedure reduces the number of nuclei to a level that will result in a ratio of ice crystals to cloud droplets (1:100 to 1:10) which will allow ice crystal growth to proceed without greatly depleting available cloud water in the ICC. This procedure also prevents the generation of transient supersaturations which can occur when warm, moist air is injected into the cloud. For conditions where ice nucleation activity is low (e.g., warmest supercooled temperatures), it is necessary to inject undiluted samples.

The primary focus of this study involved the generation and characterization of the ice nucleating ability of aerosols produced from the combustion of acetone-water solutions consisting of 2% AgI by weight and 0.50 mole of NH_4I (ammonium iodide) with respect to AgI. The ground-based generators used were the Montana State University Skyfire-type generator (MSU) and the North American Weather Consultants (Salt Lake City, UT) ground generator (NAWC). In addition, some selected experiments were performed burning 3 weight % solutions of composition AgI-0.5NH_4I-acetone-water in the MSU generator and 2% AgI solutions of composition AgI-0.385NH_4I-0.125NaI-0.2175$C_6H_4Cl_2$ -acetone-water in the NAWC generator. The former of these two solutions was burned in the past in the MSU generator and provides a check versus results obtained at CSU during 1972. The latter solution containing NaI (sodium iodide) and $C_6H_4Cl_2$ (paradichlorobenzene) is a means for producing condensation-freezing ice nuclei of expected composition AgICl-0.125NaCl. The speed of this condensation-freezing ice formation process was of particular interest.

The wind tunnel provides for aerosol generation with or without the use of a high capacity axial fan. Natural wind flow through air vents below the tunnel area and the heat of combustion was used to provide a "natural" draft for carrying effluent up the tunnel. The inability currently to define the exact flow in every natural draft situation is a potential source of the variability between tests at the same set of conditions. For these tests, as for past tests at the Sim Lab, a constant volume flow of $1x10^5$ liters per minute is assumed for natural draft conditions (Garvey, 1975; DeMott et al., 1983). This represents a flow of 2-3 m s^{-1} (measured by a hot wire anemometer) within the tunnel and essentially calm conditions at the generator heads. The 2% AgI solutions were also burned in both generators for conditions of maximum fan displacement. This resulted in a volume flow rate of $3.23x10^6$ liters per minute in the tunnel, representing about 55 m s^{-1} wind velocity. In the burning area beneath the tunnel the wind velocity is about 10m s^{-1} past the generator heads. While this was intended to simulate aerosol generation during strong surface wind conditions during storm episodes, the flow past the generator heads was more vertically-oriented rather than horizontally-oriented. Nevertheless, the expected

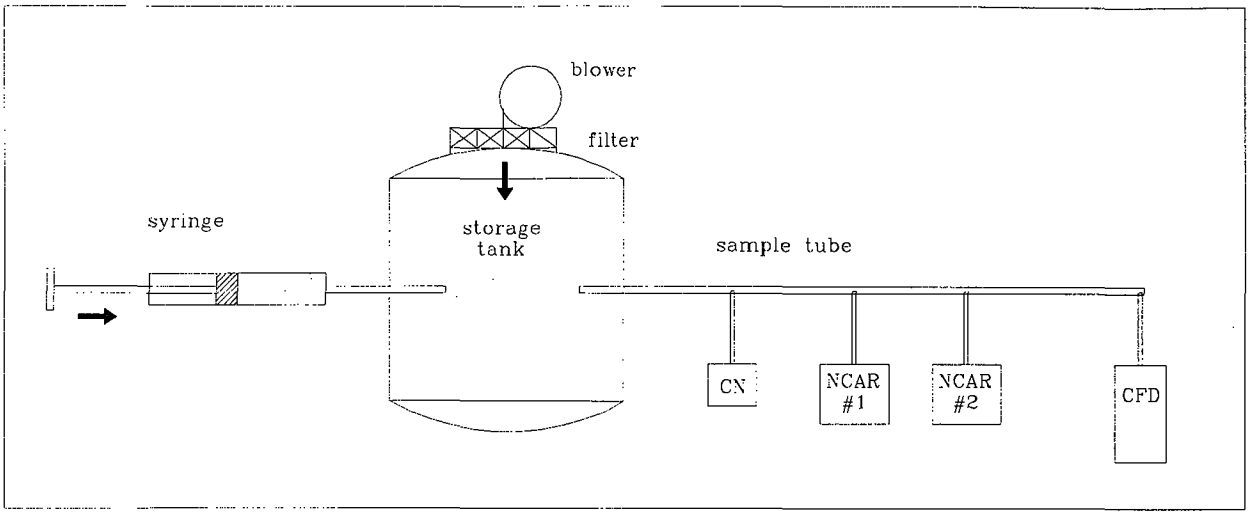

Figure 1. Schematic of aerosol sampling system.

quenching of the burn was simulated and the effect on ice formation was investigated. Both generators were operated with their wind shields in place.

Solution flow rates were characterized prior to testing at CSU. The burn rates for 2% AgI-0.5NH_4I solutions were 0.33 g min^{-1} for the MSU generator and 0.13 g AgI min^{-1} for the NAWC generator. The burn rate for the 3% AgI solution in the MSU generator was 0.50 g min^{-1}. The burn rate in the NAWC generator for the solution producing aerosol containing NaCl was assumed to be the same as for the standard 2% AgI solution. Propane was used both for pressurization (at 5 psi) and as a combustion source in the generators.

The procedures for storing aerosols for comparison between the ICC and other ice nucleus counting devices was similar to those used by Sackiw et al. (1984). A schematic of the system used is shown in Figure 1. For part of the testing program, two 4.25 liter syringe samples of aerosols were removed from the wind tunnel within a matter of seconds apart. One syringe was for use in the cloud chamber, while one was injected into a precleaned 770 liter holding tank in the laboratory. The holding tank was precleaned by blowing air into the tank through a HEPA filter. Total particle concentrations were monitored using a condensation nucleus counter (TSI Model 3010) sampling at 1 liter per minute. Immediately prior to injection of aerosols from the syringe, the blower was turned off. Residual turbulence aided in mixing particles throughout the tank. The NCAR counters, CFD and CN counter were connected to the holding tank through a 1 inch diameter copper manifold. As they drew air from the storage vessel, the air was replaced by air which flowed through the HEPA filter. This also helped to relatively quickly mix the aerosol in the tank and continually deplete concentrations in the vessel at an expected first order decay rate with rate constant 0.0273 min^{-1} (21 L min^{-1}/770L).

2.2 Isothermal Cloud Chamber

The characteristics of the isothermal cloud chamber are described in detail elsewhere (Garvey, 1975), but are briefly summarized here. The 0.96 m^3 chamber can be controlled to contain a supercooled cloud within 0.3°C a test temperature between 0 and -25°C). The liquid water content (LWC) of the cloud can be set to any value between 0.2 and 3.0 g m^{-3} by controlling the rate at which cloud droplets are continuously introduced. After aerosol injection into the cloud, the number of ice crystals collected onto a tray of microscope slides is used to determine the total number settled from the chamber. The slides are successively pulled from the bottom of the chamber at 3 to 5 minute intervals until all ice crystals are nucleated and settle out. Crystals are counted manually using a cold-stage microscope. Yield (effectiveness) is calculated as the ratio of the total number of ice crystals formed to the mass of nucleating material in the sample injected.

Ice crystal formation and fallout times can vary from 1 to 50 minutes or more depending on a number of factors, including nucleus aerosol chemistry, ice formation mechanism, humidity in excess of water saturation and temperature (DeMott et al., 1983). Rates of ice crystal formation in the isothermal cloud chamber are presented as a means of displaying the time necessary for a given percentage of the effective ice nuclei to form ice crystals. The rates presented apply only for the cloud conditions simulated. These measured rates can only be given meaning for the conditions present in natural clouds if it is possible to infer the operative mechanism(s) for ice formation. Additional details of particle size and chemistry can influence the rate at which these processes occur. Utilizing the capability to vary cloud droplet concentrations in the ICC, and simple principles of chemical kinetics (DeMott et al., 1983), it is possible to distinguish whether ice formation results primarily from a collision-dependent or collision-independent process at water saturation. If the rate at which ice appears is found to predictably depend on cloud droplet concentrations (for the same droplet mean size), it can be deduced that contact-freezing nucleation is a dominant ice formation mode. The rate of ice crystal formation in real clouds by this mode will depend on time and the droplet sizes and concentrations present. Similarly, if the rate of ice crystal formation is not found to depend on droplet concentration in the ICC, it can be presumed that nucleation is dependent on a vapor to ice or a condensation-freezing process. In this case, both activity and ice formation rate in real clouds will probably depend on both temperature and water vapor saturation ratio. Ice crystal formation kinetics were examined in this study, but a definitive statement of the mechanisms of ice crystal formation can only be made by further testing at varied temperatures and LWC.

In all, 44 experiments were conducted in the isothermal cloud chamber, spanning a number of temperatures between -6 and -20°C. LWC was set to 0.5 g m^{-3} for all experiments. This value represents about 2100 droplets cm^{-3} in the cloud chamber. This high value of droplet concentration results from the small modal diameter (~7 μm) of cloud droplets generated by the ultrasonic humidifier used. It should be remembered that the cloud produced is only intended to reproduce a supercooled cloud environment and is not a true simulation of a wintertime orographic cloud.

2.3 NCAR Ice Nucleus Counters

Two NCAR ice nucleus counters used to track the transport and dispersion of AgI aerosols in the 1994 Utah program were operated for comparison to the isothermal cloud chamber results. One counter had been deployed in an instrumented van driven on plateau-top highways, and the other was used in an aircraft. The fundamental operating characteristics of these devices are as described by Langer (1973). The two units used were built in 1976 at NCAR. The counters were tested in the same condition that they returned from the field season, except that the electronic sensitivity of the counters was reset for the Fort Collins elevation (4860 ft.). The mobile ground unit operated at about 10000 ft. and the aircraft unit was pressurized to 8000 ft. during the field program.

The NCAR counters were operated at -20°C, so comparisons to the isothermal chamber results were made at this temperature for as many of the aerosol types generated as possible. In addition, the counters were operated when testing was being conducted at -16 and -12°C in the ICC. In these cases, the ICC values were normalized to the values at -20°C for comparison to the NCAR counter. The cloud in the counters has been previously estimated to have a droplet concentration of 15000 to 20000 cm^{-3} with an average diameter of about 5 μm.

The NCAR counters sampled from the storage vessel at 10 liters per minute. The standard correction factor of 10 for ice crystals which do not make it into the NCAR counter detection section (Langer, 1973) was made to the raw data. In addition, a correction was made for coincidence losses caused by count integrators using an approximate 0.0075 s delay during each second in order to process the signal. This correction is described by the equation,

$$x_{true} = x_{obs} / (1 - (x_{obs}\, y / 60000)) \qquad (1)$$

where x_{obs} is the counter concentration value (L^{-1}), x_{true} is the corrected value and y is the counter-specific delay in milliseconds. This equation is valid for x_{obs} less than about 8000 (depends on y). No data retrieval is possible for higher count values. Concentration data were integrated and recorded at

Table 1: Yield (Effectiveness) Data for MSU Generator

Temperature	Yield		
(°C)	(#/g^{-1} AgI) AgI (2%) Natural Draft	(#/g^{-1} AgI) AgI (2%) Maximum Draft	(#/g^{-1} AgI) AgI (3%) Natural Draft
-6	$3.60X10^{10}$	$7.60X10^{11}$	$8.60X10^{10}$
-6	$8.60X10^{10}$	$2.50X10^{11}$	$5.50X10^{10}$
-8	$7.40X10^{13}$		
-8	$2.00X10^{13}$		
-12	$3.70X10^{14}$	$1.10X10^{15}$	$3.90X10^{14}$
-12	$4.90X10^{14}$	$1.00X10^{15}$	$2.30X10^{14}$
-16	$8.50X10^{14}$		
-16	$4.90X10^{14}$		
-20	$7.80X10^{14}$	$1.20X10^{16}$	$3.80X10^{14}$
-20	$6.00X10^{14}$	$4.80X10^{15}$	$3.00X10^{14}$
-20	$6.20X10^{14}$		

Table 2: Yield (Effectiveness) Data for NAWC Generator

Temperature	Yield		
(°C)	(#g^{-1} AgI) AgI(2%) Natural draft	(#g^{-1} AgI) AgI (2%) Maximum Draft	(#g^{-1} AgI) AgICl-0.125NaCl Natural draft
-6	$3.80X10^{12}$	$7.30X10^{11}$	$8.30X10^{12}$
-6	$4.80X10^{12}$	$2.50X10^{11}$	$1.30X10^{13}$
-8	$9.30X10^{13}$		$9.80X10^{13}$
-8	$1.80X10^{14}$		$8.00X10^{13}$
-12	$1.20X10^{15}$	$2.20X10^{15}$	$8.30X10^{14}$
-12	$1.50X10^{15}$	$2.90X10^{15}$	$1.00X10^{15}$
-16	$1.60X10^{15}$		
-16	$1.90X10^{15}$		
-20	$1.90X10^{15}$	$2.30X10^{16}$	
-20	$1.70X10^{15}$	$2.40X10^{16}$	

one minute intervals during sampling. The 15 liter volume of the flow-through processing chamber also causes some lag-time measurement effects, as discussed by Heimbach et al. (1977), which may lead to an underestimate of the transient peak ice nucleus concentration in the tank. Because the IN concentration changed slowly in the tank, this factor was considered minor and no correction was made. It is also possible that the short residence time (~1.5 min) in the counter leads to an underestimate of ice nuclei which require longer times for activation.

2.4 Continuous Flow Diffusion Chamber

A continuous flow ice-thermal diffusion chamber (CFD) for ice nuclei measurement was also connected to the manifold for a few selected experiments during the program. This chamber is the unit described by Rogers (1988; 1994) with some minor changes. A brief description is given here. The chamber consists of an annular gap between two ice-coated cylinders. The cylinders are held at different temperatures, and a supersaturation forms between them. The aerosol sample, ~15% of the total air flow, is smoothly injected into this space, between two equal layers of particle-free sheath air. Droplets and

crystals nucleate in the supersaturated region and grow as they pass through the first ~2/3 of the chamber. The last 1/3 has no ice on the warm cylinder; instead, it has a thin layer of dry insulation, and this change in boundary conditions creates a region that is below water saturation, so water droplets evaporate. This evaporation region helps to exaggerate the size difference between ice crystals (~5-15 μm) that formed on ice nuclei from the much smaller residues of cloud droplets (<1μm). At the chamber's outlet, the particles are counted with an optical particle counter (OPC); the amplitude of the OPC voltage pulses correspond to particle size. The pulses are digitized and accumulated in a multichannel analyzer (MCA) and recorded by computer. The detection of ice crystals, or ice nuclei, is based on particle size (>4 μm). To avoid erroneously including large non-IN aerosols, they are removed at the CFD inlet by an impactor which removes all particles larger than ~3 μm.

The sample temperature and supersaturation are independently controllable. Generally speaking, the sample temperature corresponds to the average temperature of the two walls, whereas the supersaturation corresponds to their difference. In these experiments, the maximum water supersaturation (SSw) was deliberately chosen to be very high, +10%. This was done to ensure that water saturation was exceeded, so that all CCN activated, and droplets grew quickly before reaching the evaporation section. It is a unique capability of the CFD technique to produce well defined high SSw. The existence of water supersaturation was confirmed by looking through a window in the CFD just upstream of the droplet evaporation section and seeing cloud droplets illuminated by a laser beam.

3. RESULTS AND DISCUSSION

3.1 ICC Yields (Effectivities)

Yield computations for both generators and the different solution compositions are summarized in Tables 1 and 2. The use of 2% instead of the historical 3% AgI solutions in the MSU generator leads to no degradation of ice nucleus aerosol yield at the warmest temperature tested (-6°C) and an enhanced yield at colder temperatures. The latter fact is probably due to decreased average particle size and increased total numbers of particles generated per gram of AgI burned. Yield decreases a little more than an order of magnitude as temperature increases

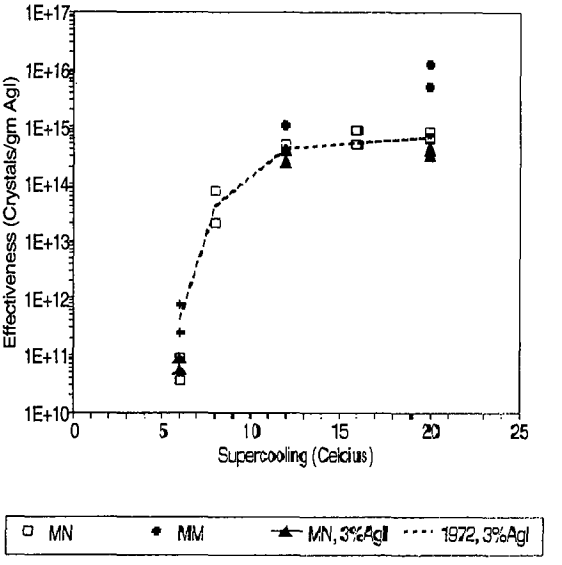

Figure 2. Yield (effectiveness) for different aerosols generated using the MSU ground generator (MN: natural draft; MM: maximum fan) as a function of cloud (LWC = 0.5 g m^{-3}) supercooling. Measurements for natural draft 3% AgI aerosols made in LWC = 1.5 g m^{-3} clouds in 1972 are also presented.

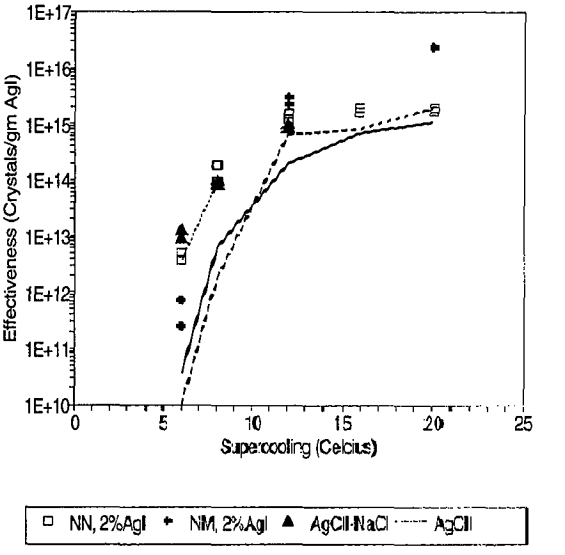

Figure 3. Yield for different aerosols generated using the NAWC ground generator (NN: natural draft; NM: maximum fan) as a function of cloud supercooling. Presented for comparison are natural draft results for 2% AgI aerosols tested in 1978 (solid line) and 1981 (dashed line), and average data points for $AgCl_{0.22}I_{0.78}$ aerosols tested in 1981.

from -20 to -8°C, but falls three more orders of magnitude lower at -6°C. Stronger ventilation of the burner leads to more rapid quenching of the flame and yet smaller and more numerous particles generated. The yield for maximum draft conditions is higher at all temperatures compared to natural draft (calm) conditions. The yield results for the MSU generator are displayed in Figure 2. The 3% AgI data from 1972 are presented for comparison. Within uncertainties which characterize ICC calibrations, the results are consistent over greater than 20 years.

Yield data for the NAWC generator tests are shown in Table 2 and Figure 3. This generator shows a slightly higher efficiency for IN generation at most temperatures compared to the MSU generator. In comparing the two generators it should be noted that the operational AgI output rate of the NAWC generator is lower by a factor of 2.5. As for the MSU generator, yield from burning 2% AgI solution decreases by about 1 order of magnitude as cloud temperature warms from -20 to -8°C. Unlike the

Table 3. Rates of Ice Crystal Formation

MSU Generator

Temp	k_{exp}	k_{dil}	k_{act}	$t_{1/e}$	$t_{90\%}$	Yield
(°C)	(min^{-1})	(min^{-1})	(min^{-1})	(min)	(min)	Correction
2%AgI-0.5 NH_4I Natural Draft						
-8	0.1162	0.0365	0.0797	12.5	28.9	1.46
-12	0.1269	0.0542	0.0727	13.8	31.7	1.75
-16	0.1696	0.0854	0.0842	11.9	27.3	2.01
-20	0.2485	0.1020	0.1465	6.8	15.7	1.70
2%AgI-0.5 NH_4I Maximum Draft						
-12	0.2302	0.0542	0.1760	5.7	13.1	1.31
-20	0.4964	0.1020	0.3944	2.5	5.8	1.26
3%AgI-0.5 NH_4I Natural Draft						
-12	0.1276	0.0542	0.0734	13.6	31.4	1.74
-20	0.2086	0.1031	0.1055	9.5	21.8	1.98

NAWC Generator

Temp	k_{exp}	k_{dil}	k_{act}	$t_{1/e}$	$t_{90\%}$	Yield
(°C)	(min^{-1})	(min^{-1})	(min^{-1})	(min)	(min)	Correction
2%AgI-0.5 NH_4I Natural Draft						
-6	0.1140	0.0302	0.0838	11.9	27.5	1.36
-8	0.1211	0.0346	0.0865	11.6	26.6	1.40
-12	0.1268	0.0474	0.0794	12.6	29.0	1.60
-16	0.1715	0.0854	0.0861	11.6	26.7	1.99
-20	0.1875	0.1057	0.0818	12.2	28.1	2.29
2%AgI-0.5 NH_4I Maximum Draft						
-12	0.2163	0.0474	0.1689	5.9	13.6	1.28
-20	0.3219	0.1057	0.2162	4.6	10.6	1.49
2%AgI-0.36 NH_4I-0.14NaI-0.15 $C_6H_4Cl_2$ Natural Draft						
-6	0.1007	0.0289	0.0718	13.9	32.1	1.40
-8	0.1373	0.0339	0.1034	9.7	22.3	1.33
-12	0.1450	0.0469	0.0981	10.2	23.5	1.48

MSU generator, yield only falls about 1.5 orders of magnitude further between -8 and -6°C, rather than 3 orders of magnitude. This result is unexpected and inconsistent with previous results obtained at CSU for this generator. Comparison of yield under natural draft generation conditions versus temperature in test series performed in different years are also compared in Figure 3. It is apparent that the generator is now producing much more efficient ice nucleus aerosols from 2% AgI solutions at -8 and -6°C. In fact, the yields at these temperatures are almost exactly those determined for AgI-AgCl ($AgCl_{0.22}I_{0.78}$) aerosols produced by adding ammonium perchlorate to the standard solution in 1981. The yield under maximum draft conditions is higher at all temperatures except -6°C compared to natural draft (calm) conditions.

The generation of AgICl-0.125NaCl aerosols using the NAWC generator had very little effect on yield, showing an increase of only a factor of 2 at -6°C, while not changing yield very much at colder temperatures. The data do suggest that measurable activity might exist for these nuclei at temperatures warmer than -6°C. The yield values obtained are consistent with values previously obtained for $AgCl_{0.22}I_{0.78}$ aerosols from the NAWC generator.

The values reported in this section are "raw" yield, as have been reported in all past calibrations. These values should be corrected for losses which are a consequence of nuclei dilution (from cloud introduction air) during the extended ice formation process. This correction requires knowledge of the rates of ice crystal formation.

3.2 ICC Rates of Ice Crystal Formation

The presentation of rates of ice crystal formation follows the conventions of DeMott et al. (1983). The plots presented in Figures 4 and 5 provide graphical depictions of the raw ice nucleation kinetics (characteristic times for effective ice nuclei depletion) for two aerosols produced by the MSU generator as observed at -12°C. The plots present the natural logarithm of [100 - % (total ice crystals formed)] versus time for two experiments. A uniform 1 minute time for ice crystal growth and sedimentation is removed from the data account for this factor which can vary from 30 to 90 s depending on temperature. A linear regression fit is drawn through the points in each case. The high linear correlation in these and all other tests suggests that the underlying process creating ice crystals is pseudo-first order and probably singular (see, DeMott et al.,

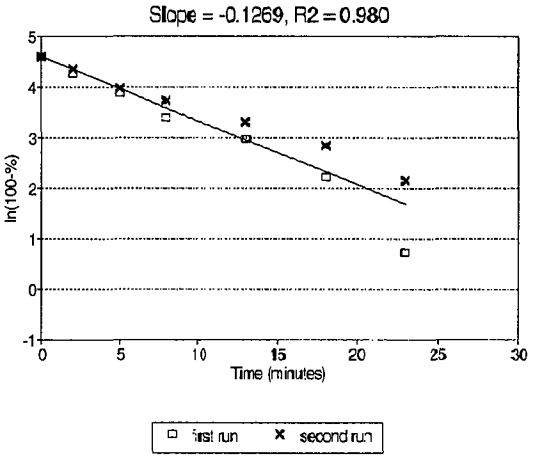

Figure 4. Ice crystal formation kinetics plot for AgI aerosols produced from combusting 2% AgI solutions in the MSU generator operating under natural draft conditions. ICC temperature was -12°C. The % in the ordinate is the percent of ice crystals formed at a given time.

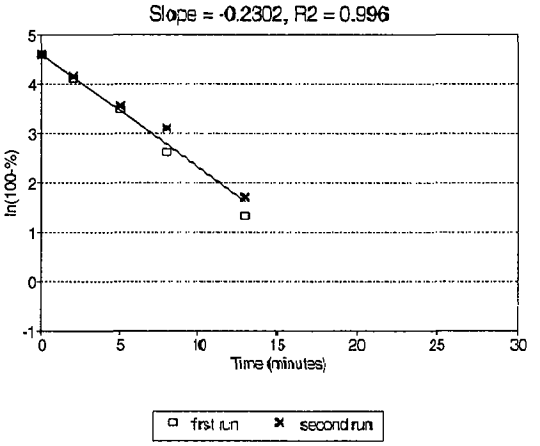

Figure 5. As in Figure 4, but for aerosols produced from combusting 2% AgI solutions under maximum draft generating conditions.

1983). The slope of the fits represents the apparent rate constant (k_{exp}) for ice formation in the chamber. These slopes are listed in Table 3 for all aerosols tested and all temperature conditions. Not enough data (ice crystal counts) were available at -6°C to reliably apply the graphical technique at this temperature in all cases. Superimposed on the ice formation process is the first-order dilution of aerosols due to air flowing into and out of the chamber to continuously supply cloud droplets. This causes nucleation rates to appear faster and nucleation yield to appear lower. The rate constant

(min^{-1}) for cloud dilution (k_{dil}), predetermined by airflow through the cloud precooling and injection pipe in particular experiments (DeMott et al., 1983), is subtracted from the apparent rate constant to obtain the true rate constants (k_{act}) in Table 3. The resultant characteristic ice formation time ($t_{1/e}$ or time to use up 63.2% of active nuclei) and the time for using up 90% of the nuclei for the cloud conditions simulated are also given in Table 3. Figure 6 shows plots of the graphically-determined characteristic times versus temperature for the different solutions tested in the two ground generators. Several points can be made regarding the rate data for each generator. For the MSU generator aerosols,

1) Ice formation times in ICC conditions were nearly independent of temperature and quite slow for natural draft aerosol generation conditions at -16°C and warmer. Rates nearly doubled at -20°C for all three solution/generation variations (Table 3 and Figure 6).

2) Strong ventilation of the generator increased rates and decreased ice formation times by a factor of 2 to 3. This is apparent on comparing the raw data in Figures 4 and 5 and the dilution corrected rate constants in Table 3 (Figure 6).

3) The use of a 3% AgI solution had little effect on ice formation rate except to slow ice formation slightly at -20°C (Table 3 and Figure 6).

These points support a conclusion of the dominance of a contact-freezing process operating for the AgI aerosols in the ICC cloud conditions, at least for temperatures of -16°C and warmer. The only obvious physical effect of increasing ventilation would be to produce more and smaller particles. An increase in ice formation rate for smaller particles within a cloud of the same droplet concentration and humidity implies a rate process limited by collisions between droplets and ice nucleus aerosols. Two additional factors support this conclusion. First, the extrapolated (versus temperature) maximum activity of the natural draft and maximum fan aerosols imply average particle diameters of 0.062 and 0.020 μm, respectively. For a collision process controlled by Brownian diffusion, calculations presented in DeMott (1990; 1995) show that the collision rate of the maximum draft aerosols with the 0.5 g m^{-3} ICC cloud should be 3.0 times faster than for natural draft aerosols. The observed value was about 3, in exact agreement. Secondly, rate results obtained for 3% AgI aerosols in 1972 (not shown) indicate that the ice formation rates in LWC = 1.5 g m^{-3} clouds

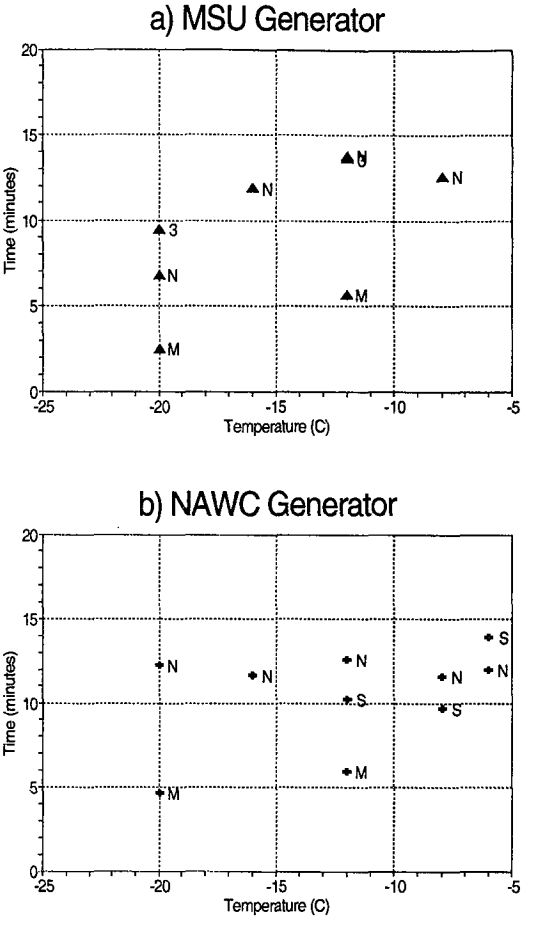

Figure 6. Characteristic (1/e) times for ice formation at different ICC cloud temperatures for different aerosols generated. Results for AgI aerosols produced from combusting 2%AgI solutions under natural draft (N) and maximum fan draft (M) conditions, AgI aerosols produced from combusting 3%AgI solutions under natural draft conditions (3), and AgICl-0.125NaCl aerosols (S) are indicated by interior labels.

containing ~4300 droplets cm^{-3} are about 2.3 times faster than for the 0.5 g m^{-3} (~2100 droplets cm^{-3}) clouds in the recent tests. Calculations estimate that the rate in the higher LWC cloud would be 2.1 times faster for a collision-controlled process, as this value should be the ratio of droplet concentration values in the respective clouds. The observations are in good agreement with calculations in both instances, considering the 30% uncertainty in droplet concentrations. Faster rates at -20°C cannot be explained in a straightforward manner for the MSU generator aerosols. It is inferred that a different or additional ice formation mechanism was operative at

this colder temperature, but it was not possible to discern what this process was.

For the aerosols produced with the NAWC generator, the following points regarding ice formation rates can be made from an analysis of Table 3 and Figure 6:

1) Ice formation rates were nearly constant and quite slow across the ICC cloud temperature range tested.

2) Strong ventilation increased rates and decreased ice formation times by a factor of 2 to 3.

3) AgICl-0.125NaCl aerosols have about 15% shorter ice formation times at temperatures colder than -8°C.

The NAWC results suggest that a contact-freezing process was also a predominant mechanism in the ICC for AgI aerosols produced from burning the standard AgI-NH_4I-acetone-water solution. Data from previous tests in 1.5 g m^{-3} clouds at CSU supports this conclusion. Previous data indicate that ice formation rates were about 2.2 times faster in the higher concentration clouds. Again, a 2.1 factor is expected for a collision-dependent process. The average particle sizes inferred from the extrapolated maximum yield in the current tests are 0.041 and 0.016 μm, respectively, for natural draft and maximum fan generation conditions. Theoretically, the collision rates of the smaller particles should be about 2 times faster than the larger ones. The maximum fan ice formation rates were observed to be 2.4 times faster than for natural draft aerosols. Thus, the data are consistent with the predominance of contact-freezing nucleation across the temperature range tested.

Inference to ice formation mechanisms by AgICl-0.125NaCl aerosols produced from the NAWC generator is difficult to make without additional information, such as varied droplet concentration tests. It was presumed that the addition of the NaI would lead to a condensation freezing process. It clearly did not result in the activation of a rapid condensation-freezing process at water saturation. As a check on the relative condensation behavior of this nucleant, some aerosols were collected and processed for CCN activity using a thermal gradient diffusion chamber (Mee Industries Model 230). The results indicated very poor CCN activity; 0.5, 2 and 5% of aerosols active as CCN, respectively, at 1, 2, and 2.5% water supersaturation. These percentage activities as CCN are almost exactly as measured for similar-sized AgI-AgCl aerosols which did not contain any NaCl (DeMott, 1990; 1995). Therefore, it is questionable whether or not the small amount of sodium chloride introduced will have any added effect toward promoting the rapid condensation-freezing process which can occur when generators are operated in ice supersaturated and subcooled wintertime situations (Finnegan and Pitter, 1988). DeMott (1991) has shown that hydrophobic AgI-AgCl aerosols will respond quite readily to the supersaturations which might occur in these situations. Nevertheless, the observation that the ice formation rate is about 15% faster than AgI aerosols at temperatures colder than -6°C suggests that the ice formation mechanism changed to condensation-freezing simply due to the slight water uptake by the $AgI_{0.78}Cl_{0.22}$-0.125NaCl aerosols. This observation is consistent with those of Finnegan et al. (1994) based on past testing at CSU using a different generator.

The rate data presented also permit correction of yield data. Since the aerosols require some time for the process of ice formation to occur, the actual yield is always somewhat higher than that given by the initial calculations presented in Section 3.1. Again, this follows from the fact that some nucleating aerosols are diluted from the chamber over time (through unsealed places) by cloud introduction air. The faster the nucleation rate, the less the correction needed. The magnitude of the correction is equal to the ratio k_{exp}/k_{act} (see, DeMott et al., 1983). This factor, given as Yield Correction in Table 3, affects one's interpretation of the effect of LWC on yield if other values of LWC are used for testing because, for a contact freezing process, the ratio is inversely dependent on LWC in the ICC. Therefore, for example, the slightly lower activity of the 3% AgI aerosols from the MSU generator in the current tests compared to the 1972 results is erased if the rate correction factors are applied.

3.3 Comparisons to NCAR Counters

Since the cross-calibration research effort was conducted in an exploratory manner, only a limited number of comparative data are considered here. A number of initial experiments were deemed to have been affected by contamination around the storage tank due to the generation of high concentrations of AgI aerosols in the nearby laboratory wind tunnel. This problem does not affect ICC calibrations because the cloud chamber room is overpressured by particle-free air, but use of the storage vessel in that room would have potentially contaminated those results. Special efforts were later taken to isolate the storage vessel from outside contamination. It was

more difficult to isolate leaks into the CN counter from around its sample inlet. Consequently, in only 3 of the tests represented in summary Table 4 were reliable CN concentrations deemed to have been recorded. Knowledge of syringe dilution conditions, generator consumption rate of AgI, and the maximum activity of the different aerosols generated as extrapolated from the ICC results were used to obtain a best estimate of initial aerosol concentration in the storage vessel. These values were used to compare to the NCAR counter and to the ICC results at -20°C. These estimated initial aerosol concentrations in the storage vessel showed good agreement with the few CN measurements which were deemed to be reliable.

Figure 7 shows an example of the response of the two NCAR counters following an injection of aerosols into the storage vessel and depicts the procedure used to calculate the initial mixed concentration value. The values presented in this figure are not corrected for coincidence losses. It can be seen that both NCAR counter records show excellent agreement after a few minutes with an exponential decay factor of 0.027 min^{-1} (represented by the solid line drawn through the data). This value of the decay constant represents the 21 liters min^{-1} being drawn from the 770 liter storage vessel and replaced with clean air. Fitting this decay curve to the data (by eye) permitted determination of the NCAR counter ice nucleus concentration at the point of injection and rejection of higher initial concentrations measured before the aerosol was completely mixed through the tank. This initial peak is exaggerated by the ~2 min. residence time of a unit sample within the counters. The two NCAR counters showed linear correlation coefficients mostly above 0.90 during the experiments, with differences generally being less than 15%.

Table 4 compares the coincidence-corrected NCAR counter ice nucleus number (NCAR in Table 4) measured for different aerosols in specific experiments with the values measured in concurrent ICC tests and with the estimated (CNEST) and measured initial CN concentration in each case. Where a different dilution factor was used in the ICC test than for the storage tank injection, the ICC value (ICC in Table 4) is corrected to be in accordance with the tank syringe dilution. The ICC value is also normalized to activity at -20°C when test temperature was different than -20°C. The correction to ICC yield for ICC airflow dilution (Tables 1 and 2) has been

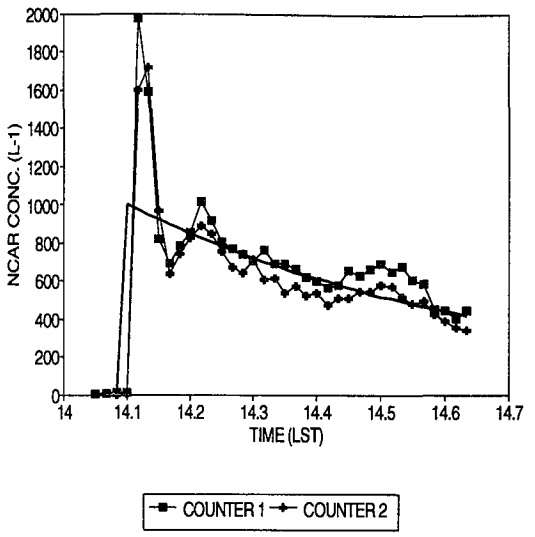

Figure 7. NCAR counter IN concentration versus time in hours local time after aerosol injection into storage vessel in one test. The decay rate caused by the 21 L min^{-1} sampling rate (solid line) is superimposed on the concentration values. The initial burst was an artifact of the mixing process.

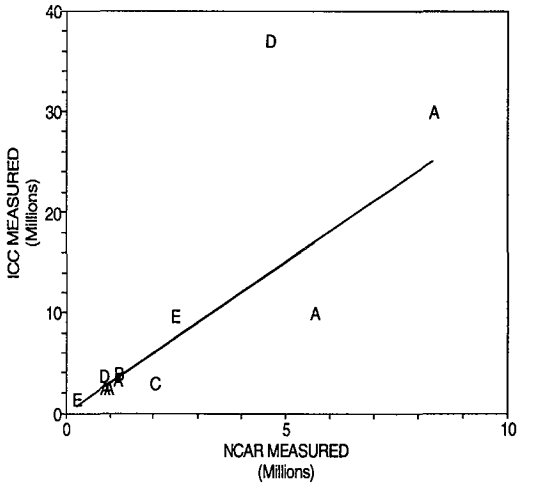

Figure 8. Dilution-corrected ICC versus NCAR counter total ice nucleus number for coordinated measurements. Following the key in Table 4, samples indicated A are the MN aerosols. The linear regression fit is for these samples. Points indicated as B, C, D, and E are for MM, MN3, NN, and NM aerosols, respectively.

Table 4. NCAR Counter/Isothermal Cloud Chamber Cross-calibration Data

CNEST	CN	NCAR	ICC	ICCC	TYPE	ICCT	NCAR/ ICCC	NCAR/ CNEST	ICCC/ CNEST
(est.)	(meas.)					(°C)			
$2.7x10^7$		$1.2X10^6$	$3.2X10^6$	$4.0X10^6$	MM	-20	**0.30**	0.04	0.15
$4.2x10^7$		$4.6X10^6$	$1.6X10^7$	$3.7X10^7$	NN	-20	**0.13**	0.11	0.88
$2.1X10^7$		$2.5X10^6$	$6.5X10^6$	$9.7X10^6$	NM	-20	**0.25**	0.12	0.46
$1.4X10^7$	$1.3X10^7$	$5.6X10^6$	$6.0X10^6$	$1.0X10^7$	MN	-20	**0.56**	0.40	0.71
$3.5X10^6$		$9.8X10^5$	$1.5X10^6$	$2.5X10^6$	MN	-20	**0.39**	0.28	0.71
$3.0X10^7$	$1.5X10^7$	$8.3X10^6$	$1.8X10^7$	$3.0X10^7$	MN	-16	**0.28**	0.28	1.00
$3.5X10^6$		$8.7X10^5$	$1.5X10^6$	$2.5X10^6$	MN	-12	**0.35**	0.25	0.71
$3.5X10^6$		$1.2X10^6$	$2.0X10^6$	$3.4X10^6$	MN	-12	**0.35**	0.34	0.97
$3.5X10^6$		$2.0X10^6$	$1.7X10^6$	$3.0X10^6$	MN3	-12	**0.68**	0.58	0.86
$4.8X10^6$		$8.6X10^5$	$1.6X10^6$	$3.7X10^6$	NN	-20	**0.23**	0.18	0.77
$2.5X10^6$		$2.4X10^6$	$6.9X10^6$	$1.4X10^7$	NM	-20	**0.17**	0.10	0.56
$4.8X10^6$			$1.6X10^6$	$2.6X10^6$	NN	-12			0.54
$3.0X10^7$	$2.7X10^7$	$1.2X10^7$			MN	-20		0.41	
					All:		**0.34**	**0.26**	**0.69**

Key:

MN: MSU generator natural draft, 2% AgI
MN3: MSU generator natural draft, 3% AgI
MM: MSU generator maximum draft, 2% AgI
NN: NAWC generator natural draft, 2% AgI
NM: NAWC generator maximum draft, 2% AgI

applied to the values listed as ICCC in Table 4. Ratios between the various quantities are also indicated in Table 4. Figure 8 presents the comparison between ICCC and NCAR for the various aerosols tested while the devices were operating concurrently. A linear regression on the data for the MSU generator aerosols generated in natural draft airflow conditions (A:MN) is given by the solid line in the figure. This fit is described by ICCC = 3.02 (NCAR) with a correlation coefficient squared of 0.87. The good correlation provides a measure of confidence in the validity of the calibration. R^2 values of 0.94 and 0.97, respectively, for linear regressions of NCAR and ICCC on CNEST for the MN data (not shown here) also validate that the two methods for measuring ice nuclei responded in kind to changes in ice nucleus concentration. The regression between the two methods suggests that the NCAR counter saw only about 33% of the MN nuclei measured by the ICC (corrected) at -20°C. A simple average of the MN NCAR/ICCC ratios gave a value of 39%. Compared to the total number of aerosols present (CNEST), the NCAR counter measured 31% on average. Compared to raw ICC values, which is the way that they are typically reported, the NCAR counters saw about 65% of the ICC-measured nuclei.

Not enough data were obtained for other aerosol types to perform complete analyses as done for the MN data. Only a single data point exists for each of the cases of a change in the wind speed or a change to 3% AgI in solutions for the MSU generator aerosols. The changes noted are an increase in the efficiency of the NCAR counters for detecting the 3% AgI aerosols and a slight decrease for detecting the 2% AgI maximum draft aerosols. It is tempting to interpret this as an effect of the differences in particle sizes in each case, but much more data would be required to confirm such an assertion. Results in Table 4 and Figure 8 also suggest that the NCAR counters are less efficient in detecting the ice nucleus aerosols from the NAWC generator. It is not clear why this should be so, but it must relate either to the inferred smaller size of the NAWC aerosols compared to the MSU aerosols or the relative efficiency of different ice formation mechanisms in the NCAR counters versus the ICC for the different aerosols.

3.4 Exploratory Studies of Ice Nucleus Behavior Using a Continuous Flow Diffusion Chamber

The CFD method has not been used before to characterize cloud seeding aerosols. These experiments provided an opportunity to explore the potential use of the instrument in this way. Only results from studies of the AgICl-0.125NaCl aerosols will be presented here. The CFD sampled during a period of simultaneous measurements with the ICC, but not while the NCAR counters were operating. The CFD sampled from the tank while the temperature and supersaturation varied continuously. Figure 9 shows the history of temperature, SSw, and SSi. Total air flow through the CFD was ~9 LPM; sample flow was ~1.5 LPM. Sample residence time within the CFD was about 5 s. The time history of IN and CN measurements are shown in Figure 10. The CN trace shows that the particle concentration in the tank was fairly steady near $1.5x10^5$ L^{-1} during this test. It decayed much slower than during the NCAR counter experiments because the airflow demand was less, 2.5 LPM instead of ~21 LPM. At the time of coldest temperatures and highest supersaturation, IN reached values of ~$5x10^4$ L^{-1}. Notice that the initial rise of IN was very rapid and was associated with SSw exceeding 0%. IN concentration increased by approximately three orders of magnitude as the temperature dropped 2°C and SSw rose to 4%. For these exploratory experiments, temperature and SSw were changed together, so these data do not clearly separate the two effects on ice formation. The ICC data indicate that at most a factor of about 2 increase in ice formation should have been expected based on temperature change alone.

The fraction of AgI aerosols that are active as ice nuclei in the CFD can be calculated by combining the IN and CN measurements. That is, the fraction active is the concentration of IN divided by the total particle concentration (CN) at each point in time. This fraction is shown in Figure 11. It is seen that more particles were activated during transit through the CFD at higher SSw, reaching maximum values of about 0.4 at 7% water supersaturation at about -16°C. IN fraction did not increase for higher supersaturations, implying that total activation was achieved for this temperature. Although this aerosol was not tested at -16°C in the ICC, the 40% activation value is about the expected aerosol fraction which can activate under any conditions at -16°C.

The CFD results for AgICl-0.125NaCl aerosols are better understood by considering ice

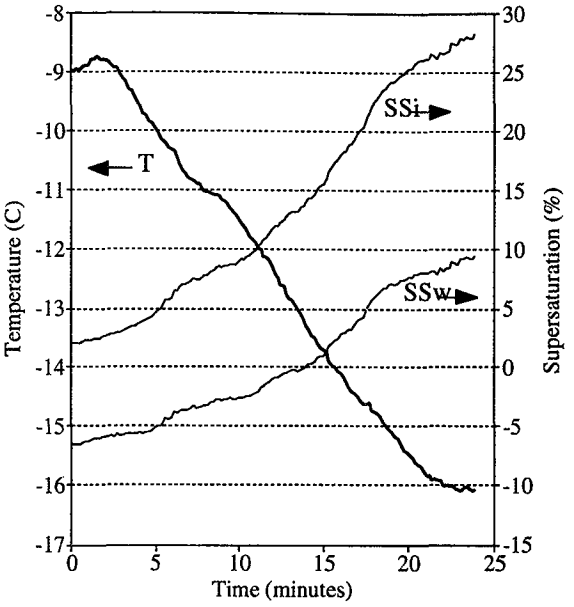

Figure 9. History of temperature, SSw, and SSi at the location of the AgI aerosol in the CFD.

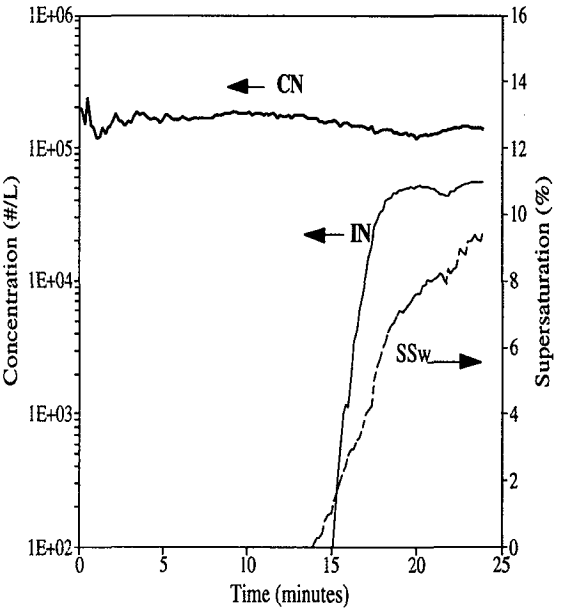

Figure 10. History of particle concentrations and water supersaturation in CFD experiment. Note that IN and SSw traces are in phase.

formation mechanisms. Since residence times are very short and droplet concentrations too small for contact-freezing to occur in the CFD; the primary

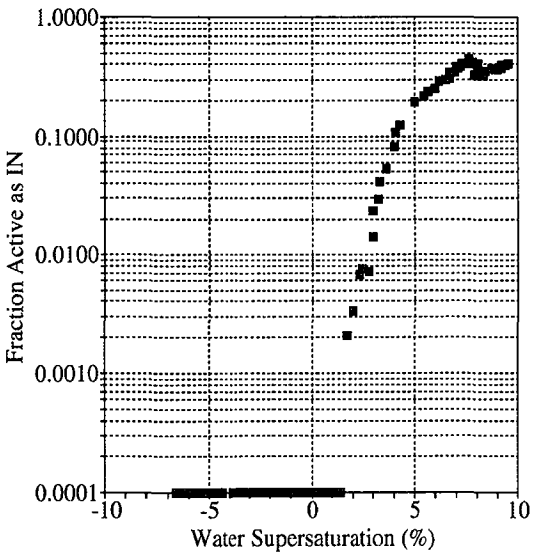

Figure 11. Fraction of aerosols active as ice nuclei versus water supersaturation. Temperature decreased from -13.6°C to -16.2°C as SSW rose from 0 to 9%. Fractions of 0 are plotted at 0.001.

mechanisms analyzed for are condensation-freezing, sorption and deposition. Since the CFD found very little activity at SSw <0%, we conclude that condensation-freezing was the primary ice formation mode measured in the CFD. The results observed are then reasonably consistent with isothermal cloud chamber results and with considerations based on the CCN characteristics of the aerosols tested. The ICC tests suggested that a condensation-freezing process predominated. The rate constant for this process measured at -12°C in the ICC was 0.00167 s^{-1}. This implies that the fraction of total aerosol number capable of forming ice in the CFD at near water saturation should have been 0.4(1-exp(-0.00167(5))) or 0.003. Here we have used 0.4 as the maximum aerosol fraction active at -16°C and a transit time through the CFD of 5 s. The expected fractional activation did not occur until SSw reached 2% in the CFD test. Nevertheless, considering that both temperature and supersaturation were changing fairly rapidly at the time of the measurement, the agreement is not bad. As SSw rose further, the ice formation rate by condensation-freezing increased until the activation was complete within the CFD transit time. That a fairly high supersaturation was required for this to occur is consistent with the high SSw required for these aerosols to act as CCN. Thus, the rate of ice formation by condensation freezing is related to the ease of formation of dilute solution droplets. This is in agreement with the observations of Feng and Finnegan (1989) that AgICl-NaCl aerosols with higher molar ratios of NaCl showed faster rates of ice crystal formation by condensation-freezing. DeMott (1990) found that AgICl-4NaCl aerosols act extremely efficiently as CCN.

Further quantitative insight into the rates and yield of ice formation as a function of both humidity and temperature could be obtained in the future by operating the CFD in a different manner than was done for this exploratory study. In particular, by varying residence time within the CFD at one temperature by changing flow rate and/or chamber length, both the rate constant and yield of ice formation could be estimated.

4. SUMMARY AND CONCLUSIONS

Yield values in the CSU isothermal cloud chamber were obtained for aerosols produced from combusting 2 and 3 weight % AgI solutions using the MSU Skyfire generator. The yields for aerosols from the 2% AgI solutions were not substantially different than for 3% AgI solutions, indicating that no added benefit exists for using 3% AgI solutions in warmer supercooled cloud conditions. Comparison of 3% AgI solution aerosols in the current tests with those tested in the MSU generator in 1972 gave excellent agreement. Ventilation of the generator at higher wind speeds increased the generator yield across the temperature spectrum tested by a factor of 2 to 10 times. This is an unusual result for most generators at the warmest temperatures since the typical effect of ventilation is more rapid quenching of the burn and production of smaller particle sizes which usually are less efficient at warmer temperatures. This may merit further investigation.

Yield values obtained using the NAWC generator indicated greatly enhanced ice formation activity warmer than -10°C for AgI-NH_4I-acetone-water solutions (2% AgI) compared to earlier tests in 1978 and 1981. Apparently, some changes to generator combustion design have been made. As a consequence, a chemical change to the solution to produce very efficient $AgI_{0.78}Cl_{0.22}$-0.125NaCl composite nuclei, produced only a slight enhancement in yield at the warmest temperature tested (-6°C). Nevertheless, these aerosols do appear to offer the potential for enhanced yield at even warmer temperatures. This would have to be verified by further testing. Ventilation of the NAWC generator at higher wind speeds was found to increase

yield by about 10 times at -20°C, but decrease the yield by 10 times at -6°C. This was consistent with results obtained in previous calibrations and is believed to reflect the dependence of activation on particle size (smaller during ventilation).

Examination of ice formation rates in the isothermal cloud chamber indicated that the 2% AgI aerosols produced by both the MSU and NAWC generators functioned by contact-freezing at temperatures warmer than -16°C in the ICC. Previous tests of the 3% AgI MSU generator aerosols for higher LWC and higher droplet concentrations in the ICC indicated faster ice formation rates in proportion to droplet concentration, quantitatively supporting this conclusion. Ice formation rates were faster at temperatures below -16°C. The ice formation mechanisms in this temperature regime could not be discerned.

Use of the solution containing ammonium iodide and paradichlorobenzene in the NAWC generator did not force a rapid condensation-freezing nucleation process at water saturation in the ICC. Nevertheless, evidence does indicate that a slower condensation-freezing process did occur. This ice formation process could provide substantial advantages in natural clouds over aerosols which realize their greatest activity as contact-freezing nuclei. This is because the ice formation rates by contact-freezing are dependent on the droplet concentration at water saturation, while the ice formation rates by condensation-freezing are not. Consider, for example, a natural orographic cloud with 100 droplets cm^{-3} of similar sizes to those in the ICC tests. In this case, the contact-freezing rate constants expected in the natural cloud for MSU and NAWC natural draft AgI aerosols are obtained by multiplying the k_{act} values in Table 3 (~0.08 min^{-1} at T≥-16°C) by the ratio of in the ICC versus natural droplet concentrations (100 cm^{-3}/2100 cm^{-3}). For a 20 minute transit time at a constant temperature through the natural cloud, this implies that only about 7% of the potential yield (Tables 1 and 2) would be realized. For NAWC AgICl-0.125NaCl aerosols, the rate constant would be 0.1 min^{-1} regardless of droplet concentrations. Thus, in 20 minutes transit at one temperature, 86% of the potential yield (Table 2) would occur. An order of magnitude difference in ice crystal formation is inferred to be possible by switching aerosols from AgI to AgICl-0.125NaCl. Future studies of these and other aerosols tested for this paper would benefit from analysis of dependence of ice formation rate on varied cloud droplet concentrations and humidities, in order to validate mechanisms.

The measurements made with two NCAR counters coordinated to sample the same aerosols used in ICC tests indicated that the NCAR counters sampled ice nucleus aerosols at about one-third of the efficiency of the ICC at -20°C after dilution airflow corrections are applied to the ICC data. In comparison to raw ICC results, such as are commonly reported from the CSU laboratory, the NCAR counters detected closer to two-thirds of the ice nuclei. There appeared to be differences in this counting efficiency factor as a function of the aerosol tested, but not enough data were collected to confirm this. Nevertheless, the counting efficiency noted is a factor of about ten higher than measured for two other NCAR counters sampling different AgI aerosols by Sackiw et al. (1984). This could be related to differences in the operating characteristics of the units tested in the earlier experiments compared to the units used in the present study. It could also relate to basic differences in the counter response to the different aerosols tested in the two studies. Although the ice formation mechanism operating within the NCAR counters is unknown for the aerosols tested, the amount of ice crystals formed compared to the ICC are reasonable if one assumes that a contact-freezing process dominated, but was limited by the shorter residence time within the counters compared to the cloud chamber.

The results of the ICC/NCAR counter cross-calibration should be extremely useful for quantifying the NCAR data in field experiment studies of cloud seeding using the aerosols tested. The excellent consistency noted between the two units tested was another positive result in this regard. We recommend cross-calibrations of the type performed here for NCAR counters before use in field operations.

The CFD experiments on AgICl-0.125NaCl aerosols from the NAWC generator yielded several interesting results which demonstrate the utility of this technique alone or in concert with other measurements of ice nuclei. The results, which by their nature did not permit contact-freezing nucleation to be observed to any degree, indicated that these aerosols required greater than 4% water supersaturation to achieve 10% instantaneous activation by condensation-freezing at -16°C. These conditions are probably met on some occasions during field generation due to the moisture released during combustion (Finnegan and Pitter, 1988). Combined with the ICC results, the CFD results also

give vital information permitting calculations of ice formation rates in real clouds. This will be the subject of future analyses and experimentation. The CFD results also show that it will be readily possible to easily and quantitatively describe differences in chemically different (e.g., more hygroscopic or more hydrophobic) ice nuclei in future experiments. Concerning the practical matter of using such an instrument simply for tracking the transport of manmade ice nuclei by aircraft, the results imply that the device should be operated at a high supersaturation to facilitate efficient detection .

Acknowledgments: The research discussed in this paper was primarily supported by the NOAA Atmospheric Modification Program in cooperation with the Utah Division of Water Resources. The NCAR counters and MSU AgI generator were supplied by the Bureau of Reclamation. CFD studies were made possible through support from NSF Grant ATM-9311606.

5. REFERENCES

DeMott, P.J., W.G. Finnegan and L.O. Grant, 1983:An application of chemical kinetic theory and methodology to characterize the ice nucleating properties of aerosols used in weather modification. *J. Clim. Appl. Meteor.*, **22**, 1190-1203.

DeMott, P.J., 1990: Quantifying ice nucleation by silver iodide aerosols. Ph.D. Dissertation. Department of Atmospheric Science, Colorado State University, Fort Collins, CO, 253 pp.

DeMott, P.J.,1991: Comments on 'The persistence of seeding effects in an orographic cloud seeded with silver iodide burned in acetone.' *J. Appl. Meteor.*, **30**, 1376-1380.

DeMott, P.J., 1995: Quantitative descriptions of ice formation mechanisms of silver iodide-type aerosols. *Atmospheric Research* [in Press].

Feng, D., and W.G. Finnegan, 1989: An efficient, fast-functioning nucleating agent -- AgI-AgCl-4NaCl. *J. Wea. Mod.*, **21**, 41-45.

Finnegan, W.G., and R.L. Pitter, 1988: Rapid ice nucleation by acetone-silver iodide generator aerosols. *J. Wea. Mod.*, **20**, 51-53.

Finnegan, W.G., A.B. Long and R.L. Pitter, 1994: Specific applications of ice nucleus aerosols in weather modification. Preprints, 6th WMO Scientific Conference on Weather Modification, Paestum, Italy, 247-250.

Garvey, D.M., 1975: Testing of cloud seeding materials at the Cloud Simulation and Aerosol Laboratory, 1971-1973. *J. Appl. Meteor.*, **14**, 883-890.

Heimbach, J.A., Jr., A.B. Super and J.T. McPartland,1977: A suggested technique for the analysis of airborne continuous ice nucleus data, *J. Appl. Meteor.*, **16**, 255-261.

Langer, G., 1973: Evaluation of NCAR ice nucleus counter. Part I: Basic operation. *J. Appl. Meteor.*, **12**, 1000-1011.

Rogers, D.C., 1988: Development of a continuous flow thermal gradient diffusion chamber for ice nucleation studies. *Atmospheric Research*, **22**, 149-181.

Rogers, D.C., 1994: Detecting ice nuclei with a continuous-flow diffusion chamber - some exploratory tests of instrument response. *J. Atmos. Oceanic Tech.*, **11**,1042-1047.

Sackiw, C.M., F.E. Robaitaille, J.W. Mason, F.D. Barlow, W.G. Finnegan, R.D. Horn and J.A. Heimbach, Jr., 1984: Comparison tests of NCAR ice nucleus counters. Ext. Abstracts of 9th Conf. on Weather Modification, 21-23 May, Park City, UT, Amer. Met. Soc., 12-13.

Super A.B., and E.W. Holroyd, 1994: Estimation of effective AgI nuclei by two methods compared with measured ice particle concentrations in seeded orographic cloud. *J. Wea. Mod.*, **26**, 33-40.